ISSN 2347-3487

MAGNETIC AND DIELECTRIC PROPERTIES OF $BiFeO_3$ NANOPARTICLES

N. Manjula[1], S. Ramu[2], K. Sunil kumar[3], D. Amaranatha Reddy[4], R.P.Vijayalakshmi[5]
[1] Research Scholar,Department of Physics, S.V. University,manju8611@gmail.com
[2] Research Scholar, Department of Physics, S.V. University,ramu.simgiri@gmail.com
[3] Research Scholar, Department of Physics, S.V. University,seelaiah786@gmail.com
[4] PDF, Department of Chemistry and Chemical Institute for Functional Materials,Pusan National University, Busan 609-735, Republic of Korea,amara123reddy@gmail.com
[5].Asso.Prof.R.P.Vijayalakshmi, Department of Physics, S.V. University,Tirupati-517502,vijayaraguru@gmail.com

ABSTRACT

Single crystalline nano-sized multiferroic $BiFeO_3$ (BFO) powders were synthesized through simple chemical co-precipitation method using polyethylene glycol (PEG) as capping agent. We obtained pure phase $BiFeO_3$ powder by controlling pH and calcination temperature. From X-ray diffraction studies the nanoparticles were unambiguously identified to have a rhombohedrally distorted perovskite structure belonging to the space group of R3c. No secondary phases were detected. It indicates single phase structure. EDX spectra indicated the appearance of three elements Bi, Fe, O in 1:1:3. From the UV-Vis diffuse reflectance spectrum, the absorption cut-off wavelength of the BFO sample is around 558nm corresponding to the energy band gap of 2.2 eV. The size (60-70 nm) and morphology of the nanoparticles have been analyzed using transmission electron microscopy (TEM). Linear M−H behaviour and slight hysteresis at lower magnetic field is observed for $BiFeO_3$ nanoparticles from Vibrating sample magnetometer studies. It indicates weak ferromagnetic behaviour at room temperature. From dielectric studies, the conductivity value is calculated from the relation $\sigma=L/R_bA\ Sm^{-1}$ and it is around 7.2×10^{-9} S/m.

KEYWORDS: Multiferroics; $BiFeO_3$; co-pricipitation method

Council for Innovative Research
Peer Review Research Publishing System
Journal: JOURNAL OF ADVANCES IN PHYSICS
Vol.7, No.2
www.cirjap.com, japeditor@gmail.com

ISSN 2347-3487

1.0 INTRODUCTION

The field of Multiferroics was born from the interest in the electric control of the magnetic properties of a system [1]. Multiferroic compounds are promising materials for the design and fabrication of multifunctional devices. They are noteworthy for their unique and storage coupling of magnetic, electric and structural parameters engenders to simultaneous ferromagnetic, ferroelectricity. Among all the multiferroic materials, $BiFeO_3$ exhibits the coexistence of ferroelectric (Tc~1103 K) and anti ferromagnetism ($T_{N\sim}$ 643 K) with weak magnetism at room temperature due to a residual moment from a canted spin structure [2]. In addition to that, it is photocatalyst due to small band gap compared to other oxide materials [3]. It is nontoxic in nature. In bulk and thin film from it is widely studied [4]. However, $BiFeO_3$ has some inherent problems such as preparation of the single phase compound, a high leakage of current, wide difference in ferroic transition temperatures (T_C/T_N) and low magnetoelectric coupling co-efficients [5,6]. On the other hand, improvement in magnetic properties without disturbing the ferroelectric properties is essential for real use in device applications.

The bulk $BiFeO_3$ has relatively lower resistivity [7] and magnetisation [8] values. Several research groups reported difficulties in synthesizing phase pure $BiFeO_3$ [9-14]. Zhonghuua et.al [15] reported single phase and high density BFO powder sintered at 650 ^oC by the spark plasma sintering process. Xuelian Yu et al reported [16] single phase BFO nanoparticles by soft chemical synthesis method after sintering at 450^oC for 2h. Qingyu Xu et.al [17] reported $Bi_{25}FeO_{39}$ impurity phase for samples sintered at 600^oC which is removed after leaching and annealing.

The difficulties of single phase $BiFeO_3$ synthesis are well known due to narrow temperature stability range of perovskite structure [18]. The $BiFeO_3$ powder samples were synthesized by the various research groups via hydrothermal method [19], sol-gel method [20], solid state reaction through leaching in 20ml of 1.0 M solution of nitric acid [3] and decomposition of the heteronuclear $Bi[Fe(CN)_6].5H_2O$ [21]. Recently, T. J. Park et al [22] and R.Mazumder et al [23] reported room temperature ferromagnetism in $BiFeO_3$ nanoparticles. The above results suggested that the $BiFeO_3$ in nano form are of exhibiting remarkable multiferroic properties. Large numbers of reports are available on $BiFeO_3$ in nano form. But the problem in synthesizing single phase is not clearly mentioned and all properties are not reported in a single paper. Hence, in this paper, we report the synthesis and properties of single phase $BiFeO_3$ nanoparticles through the simple and cost effective chemical co-precipitation method

2.0 EXPERIMENTAL

Pure $BiFeO_3$ nanoparticles were prepared by chemical co-precipitation technique using polyethylene glycol (PEG) as stabilizer. The AR grade $Bi(NO_3)_3.5H_2O$, $Fe(NO_3)_3.9H_2O$, HNO_3, $NH_3.H_2O$ were used as source materials. In typical procedure, appropriate molar proportions of Bi $(NO_3)_2.6H_2O$ and Fe $(NO_3)_2.9H_2O$ were dissolved in 100 ml of distilled water and stirred for 30 minutes. After that an ammonium solution was added to the mixed solution till the pH reached to 11. Finally PEG was added to the above mixture as stabilizer and the resultant solution was stirred for 14 hours at room temperature. Then the final solution was subsequently washed with distilled water for several times and dried at 100^oC for 5 hours. The obtained samples were grinded by using agate mortar. Finally as-prepared nanoparticles were annealed at 600^oC for 2 hours.

Crystalline structure of the $BiFeO_3$ particles were obtained using an X-ray diffractometer (model-3003TT) with Cu Kα radiation source (Wavelength, λ=1.5420 Å) in the 2ɵ range of 20^0-80^0 with a scan rate of 1^0/min. The sample composition was obtained by Energy dispersive X-ray (EDAX) analysis. The particle size and structural studies has been carried out using transmission electron microscopy (TEM), and high-resolution TEM (HRTEM) of Hitachi-H7650. Raman scattering measurements were carried out at room temperature using a JY Labram HR800 Raman spectrometer in backscattering geometry. The magnetization of the BFO powders was carried out by using vibrating sample magnetometer (VSM) integrated in a physical property measurement system (PPMS-9, Quantum Design). Dielctric and conductivity studies were carried out using Impedance Analyzer (Model) solatron (SI 1260) General a.c circuit theory.

3.0 RESULTS AND DISCUSSION

3.1 Compositional analysis

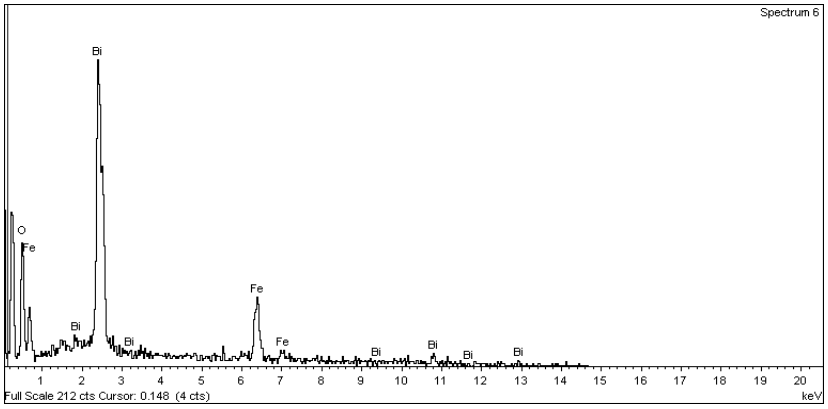

Fig. 1. EDAX spectrum of $BiFeO_3$ nanoparticles

ISSN 2347-3487

The sintered $BiFeO_3$ nanoparticles were subjected to chemical analysis using energy dispersive analysis of X-rays (EDAX) technique and is shown in Fig 1.The signals of O, Bi and Fe elements were marked in Fig 1, the EDS analysis confirms that the chemical composition of Bi, Fe and O in BFO are in the ratio 1:1:3. These results are in agreement with the reported values of Simant Kumar Srivastav and Namdeo [24-26].

3.2. Structural studies

The XRD patterns of the $BiFeO_3$ nanoparticles sintered (at 400^oC and 600^oC) $BiFeO_3$ were shown in Fig 2(a)&(b). The prominent peaks in the XRD pattern of nanoparticles synthesized at 400^oC are indexed to (101), (012),(110), (003), (021), (202), (113), (104),(122),(024) and (220) planes of rhombohedrally distorted perovskite structure of BFO (JCPDS:20-0169 R3c space group), indicating the formation of BFO. Besides these, some other peaks of low intensity were also observed, which do not belong to BFO. The literature survey of BFO synthesis relates these peaks to be that of $Bi_2Fe_4O_9$ and Fe_2O_3 phases and presence of impurity phase of $Bi_2Fe_4O_9$ has been reported by several authors [27-28]. However, nanoparticles sintered at 600 ^0C resulted in the removal of these impurity peaks and only prominent peaks of pure BFO phase were appeared in the spectra. These results are in agreement with the earlier reports [29-30]. This implies that a single phase of BFO nanoparticles could be obtained only after sintering at 600 ^0C for 2hrs. But H. Shokrollahi [31] reported presence of impurity phases for sample synthesized at 675,750 and 825^oC by chemical co-precipitation method.

The lattice parameters a and c were calculated by using the relation $\sin^2\Theta = \lambda^2/3a^2 (h^2+hk+K^2) + \lambda^2l^2/4c^2$, where Θ is Bragg angle [32]. The grain size is calculated by Debye Scherer's equation, $Dp = 0.94\lambda/\beta\cos\theta$, where λ is the X-ray wavelength, β is the full width at half maximum of the intensity peak at the diffraction angle Θ, unit cell volume and lattice parameters are shown in Table 1.

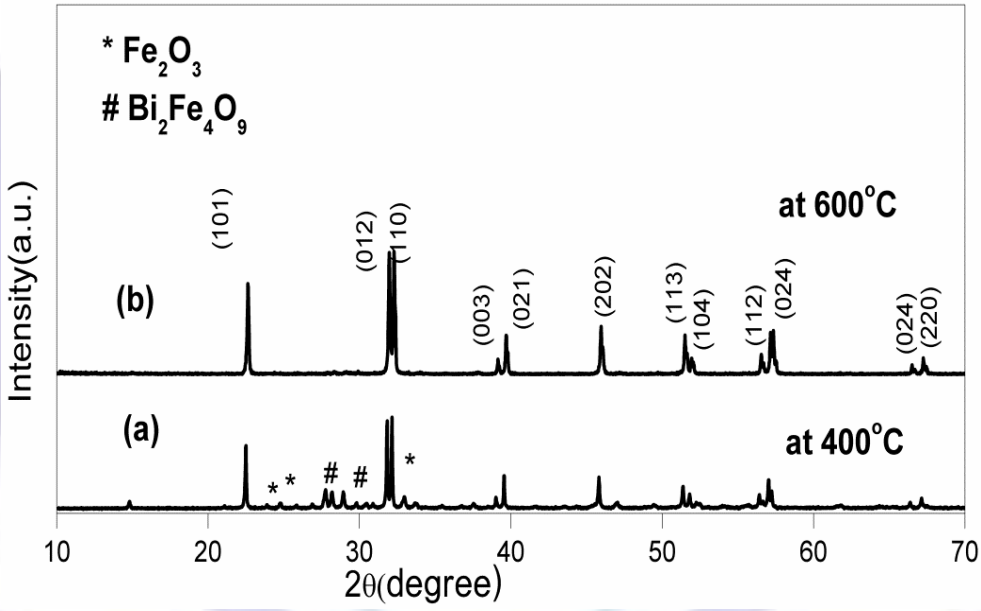

Fig 2(a). XRD spectrum of $BiFeO_3$ nanoparticles at 400^o **(b).** at 600^{o}C

Table 1

S.NO	X	a(A^0)	c(A^0)	c/a	Cell volume	Grain Size (nm)
1	0.000	5.538	6.886	1.243	548.625	63

ISSN 2347-3487

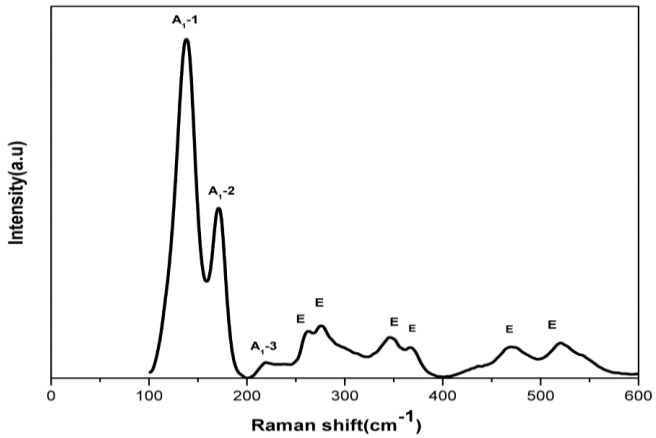

Fig 3. Raman spectrum of $BiFeO_3$ nanoparticles.

Raman spectroscopy was used to study the structural characteristics of BFO nanoparticles prepared by chemical route. The room temperature Raman spectrum of BFO nanoparticle is shown in Fig 3. According to group theory analysis, BFO should have distorted rhombohedral structure with R3c space group. Hence, BFO permits 13 active phonons summarized in the irreducible representation:$\Gamma=4A_1+9E$ [33-36]. From Fig 3 three intense peaks are observed at (137, 171, 218cm^{-1}) and six weak intense peaks are at (261,274,344,366,468,657 cm^{-1}). Similar types of vibrational modes were observed by Zhen wen, Xuan shen et al., on single crystal BFO synthesized by sol-gel method [37]. These frequency modes are in good agreement with previous reports on single crystal BFO [38] and thin films [39] are shown in Table 2.

Table 2. Comparison of Raman Mode positions (cm^{-1}) in our study with the reported data on single crystal BFO by Fukumura et al. [38] and data on thin film of BFO by Singh et al. [39].

Raman modes	Our study (cm^{-1})	Fukumura et al. (cm^{-1})	Singh et al. (cm^{-1})
A_1-1	137	147	136
A_1-2	171	176	168
A_1-3	218	227	211
E-1	261	265	275
E-2	274	279	335
E-3	344	351	365
E-4	366	375	456
E-5	468	437	549
E-6	657	525	597

3.3.TEM analysis

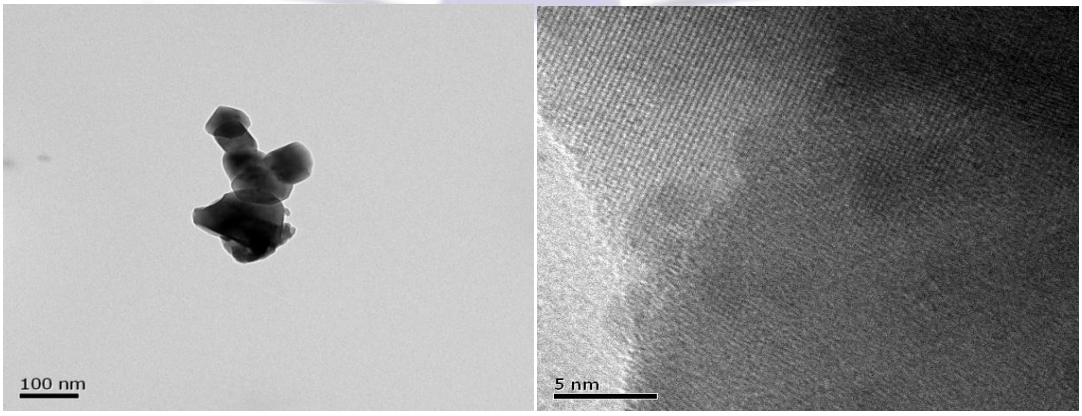

Fig 4 (a, b) TEM and HRTEM images of $BiFeO_3$ nanopartcles.

ISSN 2347-3487

The crystalline structure of the $BiFeO_3$ nanoparticles was observed by transmission electron microscopy (TEM) and is shown in fig.2(a). From the spectra it is noted that the particle size is around 60nm, it is same as the crystalline size obtained from XRD. These particles are nearly spherical in shape. The larger size of the particles may be due to the agglomeration as the particles were sintered at 600^{o}C for 2 hours. The agglomeration of nanoparticles is also reported by earlier workers [40-41]. The rhombohedral perovskite structure of the $BiFeO_3$ nanoparticles were confirmed by HRTEM (Fig 2 b).

3.4 Optical studies

It is well known that the properties of diffuse reflectance spectra are relevant to the electronic structure features and hence are the key factors in determining their band gaps. The DRS spectra for samples sintered at 600 ^{0}C are recorded and the band gap values were calculated by plotting the square of the Kubelka–Munk function [42] (F (R) ^{2}) versus Energy and extrapolating the linear part of the curve to F $(R)^2 = 0$ and is shown in fig 5. The obtained band gap is 2.2eV. This is in good agreement with the earlier reported values [43-46].

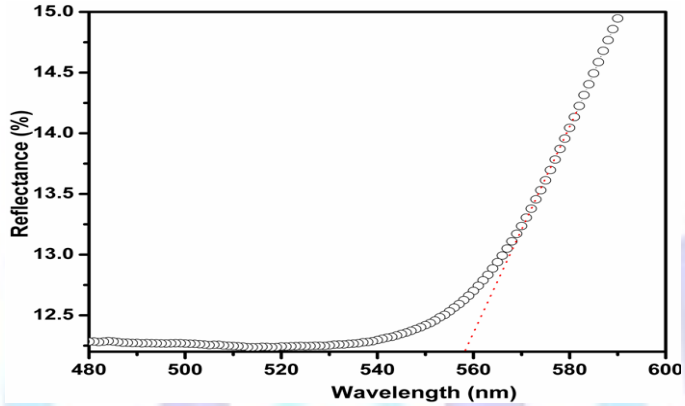

Fig 5. UV-Vis diffuse reflectance spectroscopy of $BiFeO_3$ nanoparticles

3.5. Magnetic properties

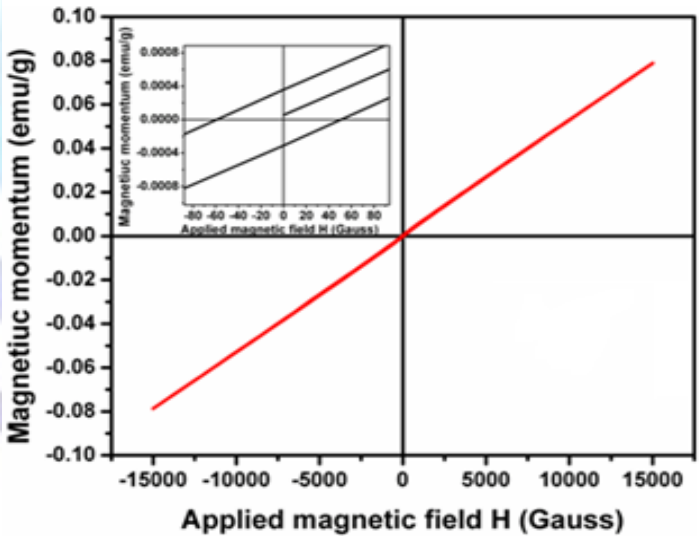

Fig 6 Room temperature M-H curve of BFO nanoparticles

Fig 6 shows the magnetization verses magnetic field (M-H) curve for $BiFeO_3$ nanoparticles carriedout at room temperature by using the vibrating samples magnetometer. From the figure it is noticed that the magnetization is linear with magnetic field. But at lower magnetic fields slight hysteresis behaviour was observed , it is shown as insite in Fig 6. $BiFeO_3$ is known to be antiferromagnetic with a *G*-type magnetic structure but has a residual magnetic moment due to a canted spin structure [47]. Wang et.al [48] also observed same type of behaviour in nano paticles from solgel method. This is attributed to the emergent of feromagnetic component in an anti ferromagnetic matrix.

ISSN 2347-3487

3.6 Dielectric properties

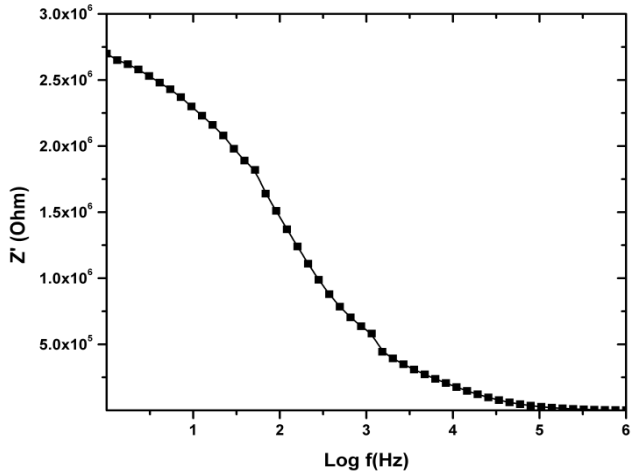

Fig 7(a) Real part of impedance with respect to frequency for $BiFeO_3$

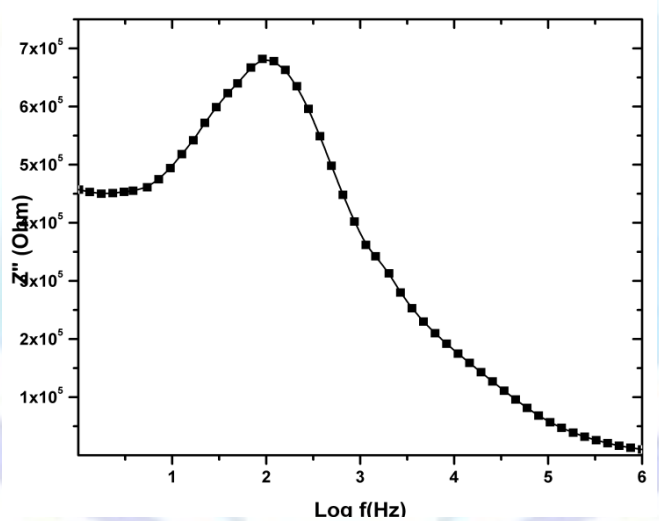

Fig 7(b) Imaginary part of impedance with respect to frequency for $BiFeO_3$.

The response of the real components of impedance (Z') with frequency at room temperature for $BiFeO_3$ is shown in Fig 7 (a)&(b). At higher frequencies > 10^3 Hz, Z' is almost independent of frequency, which is attributed to the resistance effect. In the frequency range (1Hz-10^3Hz) between these limits, Z' considerably decreases as the frequency increases. However, for the frequencies < 10^3 Hz, Z' decreases, implying a decrease in the total resistance of the sample**.** Fig 7(b) shows the variation of imaginary component of impedance (Z") with frequency for $BiFeO_3$. The relaxation or Debye-type peaks in the low frequency region and the peak intensity is found to decrease as the frequency increases.

ISSN 2347-3487

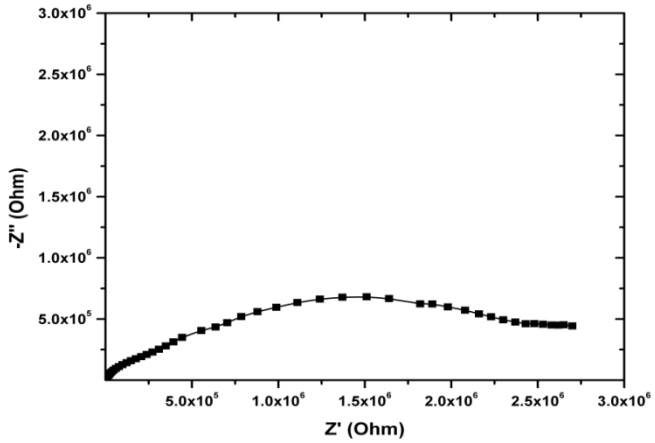

Fig 7(c). Cole-Cole plot of $BiFeO_3$.

The Cole-Cole plot for $BiFeO_3$ is shown in Fig 7(c). This plots gives information about different scattering mechanisms corresponding to different relaxation times. From the fig it was evident that the radii of semicircle pattern decreasing with increasing resistance, which indicates decrease in the total resistance of the sample and this explains the decrease of Z' and Z" as shown in Fig 7(a) and Fig 7(b).

The bulk conductivity (σ) value has been calculated using the formula [49],

$$\sigma = L/R_bA \ S\ m^{-1} \quad (1)$$

Where, R_b is bulk resistance of the sample

L is the thickness of the pellet

A is the effective area.

The conductivity values are calculated from the above relation and it is observed that the 7.2×10^{-9} S/m.

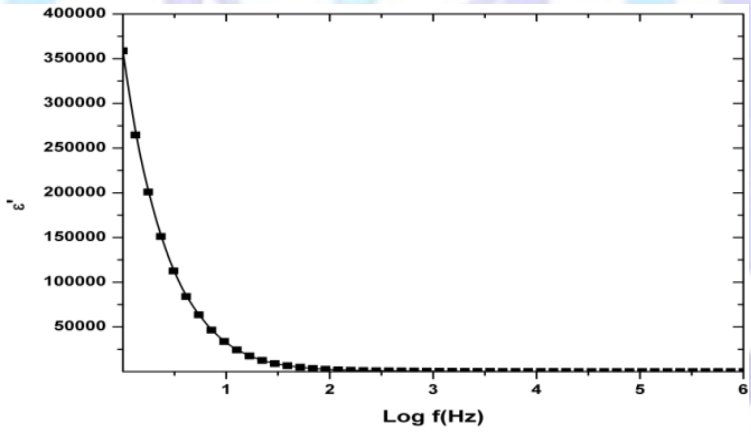

Fig 7(d). Dielectric constant with respect to frequency for $BiFeO_3$

ISSN 2347-3487

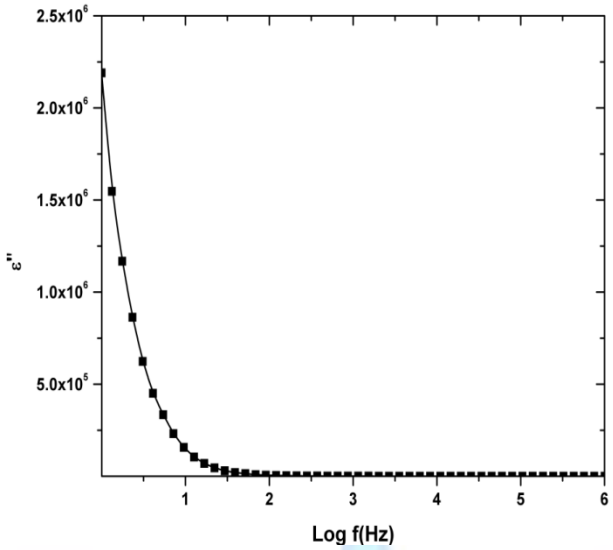

Fig 7(e). Dielectric loss with respect to frequency $BiFeO_3$

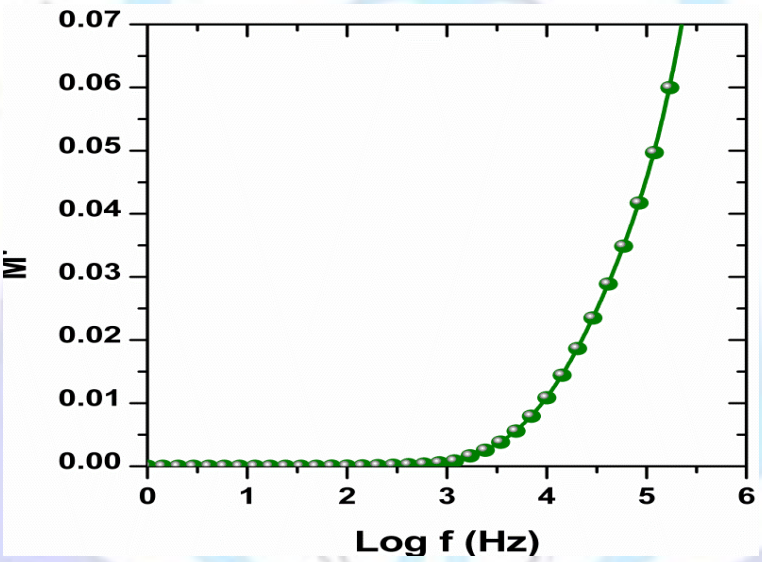

Fig 7(f). Real part of electric modulus of $BiFeO_3$.

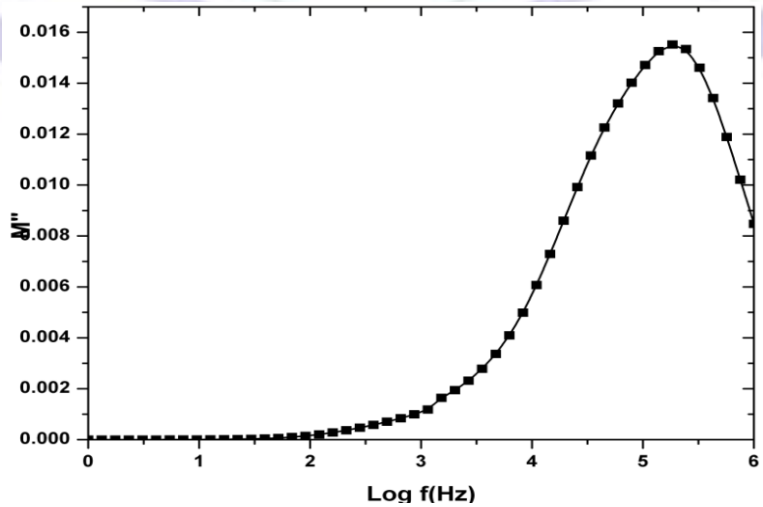

Fig 7(g). Imaginary part of electric modulus of $BiFeO_3$

The real part of dielectric permittivity or dielectric constant, ε' and imaginary part of dielectric permittivity or dielectric loss of $BiFeO_3$ measured in the frequency range 1 Hz to 1MHz is shown in Fig 7(d) and Fig 7(e). It is observed that the dielectric constant, ε' (□) of $BiFeO_3$ is decreased rapidly at lower frequencies and showed almost frequency independent behaviour at higher frequency region. It is the typical behaviour of ferrites [50-51]. The bulk polarization of the sample results from the presence of electrodes, which do not allow transfer of the charge species into the external circuit. The behaviour of the dielectric permittivity with frequency is related to the applied field, which assists electron hopping between two different sites of the sample. At higher frequency region, the charge carriers will no longer be able to rotate sufficient rapidly, so their oscillation will begin to lay behind this field resulting in a decrease of dielectric permittivity, ε' (□). Generally, the relaxation phenomena in dielectric materials are associated with frequency dependent orientational polarization. At low frequency region, the permanent dipoles align themselves along the field and contribute fully to the total polarization of the dielectric. At higher frequency region, the variation in the field is very rapid for the dipoles to align themselves, so their contribution to the polarization and hence, to dielectric permittivity can become negligible. Therefore, the dielectric permittivity, ε' (□) decreases with increasing frequency. The decrease of the dielectric constant ε'can also explain from interfacial polarization. The interfacial polarization arises as a result of difference in conducting phase, but is interrupted at grain boundary due to lower conductivity. The magnitude of the dielectric constant is also observed to be decreased. The frequency dependence of dielectric loss ε'' (□) is shown in Fig 7(e). It is observed that the dielectric loss ε'' (□) is also decreased by increasing frequency. Generally, the dielectric losses at high frequencies are much lower than those occurring at lower frequencies at specific temperature. This kind of dependence of ε'' (□) on frequency is typically associated with losses by conduction [52-53]. M. Muneeswaran et al., have reported the decrease of dielectric constant and dielectric loss gradually as the frequency increased. When the frequency increased the dielectric constant becomes weak [54].

An alternate approach to analyze electrical relaxation is electric modulus. The electric modulus M* can be defined in terms of the reciprocal of the complex dielectric constant ε *(□) as

$$M^* = 1/\varepsilon^*(\square) = M'(\square) + iM''(\square) \quad (2)$$

Where real part of complex modulus M' and imaginary part of complex modulus M" can be calculated by using following equations:

$$M' = \varepsilon'/(\varepsilon'^2 + \varepsilon''^2) \quad (3)$$

$$M'' = \varepsilon''/(\varepsilon''^2 + \varepsilon''^2) \quad (4)$$

The frequency dependence of M' (□) and M'' (□) of $BiFeO_3$ is shown in Fig 7(f) and Fig 7(g). These figures explain the relaxation nature of dielectric properties of samples. The M' (□ □□is increases with frequency and the maximum in the M'' (□ □ □shifts towards higher frequency region. The frequency above peak maximum M'' (□ □ □determines the range in which charge carriers are mobile on long distances. For frequencies higher than M'' peak frequency, the carriers are spatially confined to potential wells and being mobile on short distances making only localized motion within the wells.

4.0 CONCLUSIONS

In summary, multiferroic $BiFeO_3$ nanoparticles ranging from 60 nm to 70nm were successfully synthesized by the chemical co-precipitation process. Raman and XRD studies indicate that rhombohedrally distorted perovskite $BiFeO_3$ phase formed at room temperature. BFO nanoparticles have shown strong absorption at ~558 nm, arising from the bandgap absorption. Due to size confinement, $BiFeO_3$ nanoparticles have shown room temperature weak ferromagnitism. The conductivity value is calculated from the relation $\sigma=L/R_bA$ S m^{-1} and it is around 7.2 x 10^{-9} S/m. The research on these material may some new applications in the area of spintonics and water spliting, in addition to this it is simple, cost effective and easy to control.

ACKNOWLEDGEMENTS

The authors are thank ful to CSIR New Delhi for providing financial support through project No.03 (1281)/13/EMR-II.

REFERENCES

[1]. G.R Boyd, P. Kumar, and S. R. Phillpot. *arXiv preprint arXiv: 1101* (2011).

[2]. J.Wang, *Science* **299**, 1719 (2003).

[3]. A. Kevin. Mc Donnell, Nitin Wadner Kar Niall J. English, Mahfujur Rahman, Denis Dowling, *Chem phys Lett*. **572**,78 (2013).

[4] R. Andrew, Akbashev, Guannan Chen, and E. Jonathan. Spanier, *Nano Lett*. **14**, 44 (2014).

[5]. M. M. Kumar, V.R.Palkar, K.Srinivas, and S.V.Suryanarayanan, *Appl.Phys.Lett*. **76**, 2764 (2000).

[6]. V.R.Palkar,J.John, and R.Pinto, *Appl.Phys.Lett*. **80**, 1628 (2002).

[7] C. Jhin-Cyun, , W.Jenn-Ming, *Applied Phys. Lett*. **91**, (2007), 182903.

[8] Tae-Jin Park,C. Georgia , Papaethymion, J. Arthur, Viescas, R.Arnold, Mooden baugh, and S.Stanislaus , *Wong, Nano Lett*, **7,**3 (2007).

[9] B. Bhushan, D. Das, A. Priyam, N.Y. Vasanthacharya, S. Kumar, *Mater Chem Phys* **135**, 149 (2012).

[10] Liyan Zhang, Yang Yang, Shuyuan Ma, Wanju Luo, Yulong Liu, Ke Zhu, *Physica B* **407**, 494 (2012).

[11] A.A. Cristóbal, P.M. Botta, *Mater Chem Phys* **139**, 931 (2013).

[12]Zheng Wen, Xuan Shen, Di Wu, Qingyu Xub, Junling Wangc, Aidong Li, *Solid State Commun* **150**, 2081(2010).

[13] S. Acharya, S. Sutradhar, J. Mandal, K. Mukhopadhyay, A.K. Deb, P.K. Chakrabarti*, J Magn Magn Mater*. **324**, 4209(2012).

[14] Christopher S. Knee, G.Matthew , Tucker, Pascal Manuel, Shengzhen Cai, Johan Bielecki, Lars Börjesson, and Sten G. Eriksson, *Chem. Mater*. **26,** 1180 (2014).

[15] C. Yang a, C.Z.Liu a, C.M.Wanga, W.G.Zhang b, J.S.Jiang a,n, *J Magn Magn Mater* **324**, 1483 (2012).

[16] Xuelian Yua,b, Xiaoqiang Anc, *Solid State Commun* **149**, 711 (2009).

[17] Qingyu Xua, Xiaohong Zhenga, Zheng Wenb, Yi Yangc, Di Wub, Mingxiang Xua, *Solid State Commun.* **151** 624 (2011).

[18]. M. Mahesh Kumar, V.R. Palkar, K. Srinivas, S.V. Suryanarayana, *Appl. Phys. Lett*. **76**, 2764 (2000).

[19] Linfeng Fei, Jikang Yuan, Yongming Hu, Changzheng Wu, Junling Wang, and Yu Wang, *Cryst. Growth Des.* **11**, 1049 (2011).

[20]. Gurmeet Singh Lotey, N.K. Verma, *Chem Phys Lett* **574**,71 (2013).

[21]. Saeid Farhadi, Nazanin Rashidi, *Polyhedron* **29**, 2959(2010).

[22].T.J.Park, G.C.Papaefthymiou, A.J.Viescas,A.R. Moodenbaugh, and S.S.Wong, *Nano Lett*. **7** ,766 (2007).

[23]. R. Mazumder,D.P.Sujatha, D.Bhattacharya, P.Choudhury, A.Sen, and M.Raja, *Appl.Phys.Lett*. **91**, 062510(2007).

[24] Simant Kumar Srivastav and Namdeo, *J.Am.Ceram.Soc*., **95**, 3678(2012).

[25] M.B.Bellaki, V.Manivannan, *J. Matter. Sci*. **45,** 1137(2010).

[26] A. Mukherjee , M. Banerjee , *Physica B* **448**, 199(2014).

[27] I.Sosnowska,W.Schafer, W.Kockelmann, K.H.Andersen nd I.O.Troyanchuk, *Appl.phys. A*, **74**, 1040 (2002).

[28] Zhiwu chen and yongpeng, *J.Am.Cream.soc*., **96,** 345(2013).

[29] Saeid farhadi, Nazanin Rashidi, *Polyhedron*, **29**, 2959 (2009).

[30] M.M.Rashad, *J Mater Sci:Mater Electron* **23**, 882(2012).

[31] H.Shokrollahi, *Powder technol*, **235**,1 953 (2013).

[32] B.D. Cullity, S.Stock, Elements of X-ray Diffraction, 3rd ed., Prentice Hall, NJ, (2001) p.303.

[33]D.Kothari,V.R.Reddy,A.Gupta,V.Sathe,A.Banerjee,S.M.Gupta,A.M.Awasthi, *Appl.Phys.Lett*. **91** (2007).

[34]Y.Wang,C.-W.Nan, *J.Appl.Phys*.**103**,114104 (2008).

[35] Y.Yang,J.Y.Sun,K.Zhu,Y.L.Liu, *J.Chen,X.R.Xing, PhysicaB* **404,**171(2009).

[36] R.Palai,H.Schmid,J.F.Scott,R.S.Katiyar, *Phys.Rev.B* **81**, 064110 (2010).

[37] Zheng wen, Xuan shen , *Solid state commun*,**150**,2081(2010).

[38].H. Fukumura, S.Matsui,H. Harima, T.Takahashi,T. Itoh, K.Kisoda, M.Tamada, Y.Noguchi, M. Miyayama, *J. Phys.Condens. Matter* **19,** 365224 (2007).

[39]. M.K. Singh., H.M. Jang., S. Ryu., M.H ,Jo, *Appl. Phys. Lett.* **88,** 42907 (2006).

[40] Samar Layek , *Adv. Mat. Lett*. **3** 533(2012).

[41]. SM.Selbach, T.Tybell ,MA. Einarsrud ,T. Grande, *Chem Mater* **19(26)** ,6478(2007).

[42] . J.Tauc, A.Menth , States in the gap, *J Non.Crystal. Soli.* **8-10**,569 (1972).

[43] F.Gao, X.Chen ,K.Yin, S.Dong, *Adv.Mater*.**19,** 2889 (2007).

[44] U.A.Joshi,J.S.Jang,P.H.Borse, and J.S.Lee, *Appl.Phys.Lett*. **92** ,242106 (2008).

[45] J.Lou and P.A.Maggard, *Adv. Mater*.**18**, 2325(2006).

[46] F.Gao,X.Y.Chen,K.B.Yin,S.Dong,Z.F.Ren, F.Yuan,T.Yu, Z.G.Zou, and J.M.Liu, *Adv.Mater*. **19**, 2889(2007).

[47] T. Kanai, S.-I. Ohkoshi, A. Nakajima, T. Watanabe, and K. Hashimoto, Weinheim, Ger, *Adv. Mater*. **13**, 487(2001).

[48] Y.Wang,C.W.Nan, *J.Appl.Phys*. **103** 114104 (2008).

[49]. DP. Almond, AR.West, *Solid State Ionics*. **227**, 2738 (1987).

[50]. M.A. El-Hiti, J.*Phys III (France).* **6** 1307(1996).

[51]. A.V.R. Reddy, G.R. Mohan, D. Ravinder, B.S. Boyanar, *J. Mater. Sci.* **34,** 3169 (1999).

[52]. K.S. Cole, R.H. Cole, *J.Chem.Phys*. **9,** 341(1999).

[53]. K.S. Cole, R.H. Cole, *J.Chem.Phys.***10**, 98(1942).

[54] M.Muneeswaran, P.Jegatheesan, N.V. Giridharan, *J.Exp.Nano Sci.***8**,341(2013).